# Raman Microimaging Study of Interfacial Profiles of Hydrogels

**T. W. ZERDA,[1] RAINER APPEL,[1] ZHIBING HU[2]**

[1] Department of Physics, Texas Christian University, Fort Worth, Texas 76129

[2] Department of Physics, University of North Texas, Denton, Texas 76203

*Received 20 November 2000; accepted 25 January 2001*

**ABSTRACT:** A Raman microimaging technique was used to directly observe the interfacial profile between *N*-isopropylacrylamide (NIPA) and polyacrylamide (PAAM) hydrogels in water. The joined hydrogels are called bigels and are synthesized by penetrating the PAAM gel into a part of the NIPA gel network. The bigel strip contains about 97 wt % water at room temperature. The study reveals how different manufacturing parameters, such as the drying time of the NIPA substrate and the diffusion time of the PAAM pregel solution into the NIPA layer, influence the properties and extent of the bigel interface. The interface becomes thicker with increased drying time. Specifically, the average interfacial thickness of the interface after 2 h of drying is about 28 $\mu$m, but increases to 156 $\mu$m after 16 h of drying time. The extent of the interface is independent of the PAAM diffusion time. The penetration of the PAAM pregel solution into the pores of the NIPA gel is completed in less than 30 min. The topography of the surface can be well characterized by a Gaussian function with the correlation length describing the size of the interfacial region. © 2001 John Wiley & Sons, Inc. J Appl Polym Sci 82: 1040–1046, 2001

**Key words:** raman confocal microscopy; concentration profiles; hydrogel; interface

## INTRODUCTION

Many applications of hydrogels depend upon physical, chemical, and biological interactions of molecules at their surfaces or interfaces.[1–3] Modified surfaces could increase or decrease the hydrophilic character, pH, and permeation of molecules of the hydrogels.[1] Basic methods include coating, surface grafting, interpenetrating, and ion implantation.[2] One important goal is to develop a new generation of a superabsorbent polymer by applying a second crosslinker on the surface of the particles that are lightly crosslinked superabsorbent polymer.[4] These surface-treated particles can increase absorbency under load and suction power.

It is crucial to characterize the microstructure of surfaces or interfaces of hydrogels. This task is not easy because hydrogels contain a large fraction of water within their structures. This fraction can easily range from 92 to 99 wt %.[3] It is difficult to remove water while keeping the polymer network structure intact so that the gel can be put into a vacuum chamber for various analyses, such as electron microscopy (TEM and SEM) or electron spectroscopy for chemical analysis (ESCA). For example, the freeze-drying or super-

*Correspondence to:* T. W. Zerda.

Contract grant sponsor: Donors of the Petroleum Research Fund.

Contract grant sponsor: U.S. Army Research Office; contract grant number: DAAH04-93-G-0215.

Journal of Applied Polymer Science, Vol. 82, 1040–1046 (2001)

critical drying methods often lead to the collapse of the pore structure due to ice formation and/or volatile evaporation in a vacuum.[5] Furthermore, long-time exposure of the hydrogels to the radiation of probes such as X-ray and electron beam may alter the surface and make the results unreliable.

Here, we demonstrate that Raman microscopy can be used to directly and nonintrusively measure the interface profiles of hydrogels. Raman microimaging is based on measurements of vibrations of polymers and relating it to polymer concentration. This technique was recently applied to characterize the structure of a macroporous NIPA gel and the surface interfacial profiles of an NIPA gel in water below and above its phase-transition temperature.[6,7] In this study, interfacial profiles of bigel strips were investigated using the Raman microimaging method. The bigel strip is made by allowing the PAAM gel to penetrate into the porous NIPA gel network.[8–10] Since the NIPA gel is sensitive to temperature and the PAAM gel is sensitive to acetone concentration, the bigel can bend to an arc in response to temperature or solvent changes. Because the difference of the magnitude of the changes between the two sides of the bigels is enormous, the bending effect is much larger than is the bending induced either by an electric field[11] or by infrared light.[12] The interface of the bigel plays a crucial role in its performance. The polymer concentration gradient reaches its maximum value along the interfacial region and results in high stresses within the two polymer networks, making the interface between the two components the weakest feature in the bigels. Relatively small strains applied in the direction parallel to the interface may result in the separation of the bigel into two parts. Such separations are often observed after significant bigel bending.

The goals of this study were twofold: first, to demonstrate that Raman microscopy can be used to measure the interfacial profile of the hydrogel with a high water content, and second, to check if the interfacial profiles can be correlated with the synthesis conditions. This could result in high-performance responsive hydrogels for sensor and device applications.[13–15]

## EXPERIMENTAL

The bigel strips are synthesized by first making an NIPA gel slab. Two glass slides with a ~2.0-mm gap between them are immersed in 100 mL of an aqueous solution of 690 m*M* NIPA, 8.6 m*M* methylenebisacrylamide (BIS), and 8 m*M* sodium acrylate. The polymerization of the solution is initiated by the addition of 240 $\mu$L of tetramethylethylenediamine and 40 mg of ammonium persulfate.[16]

The resultant gels were placed in a container that was covered with a plastic film with several holes poked by a needle. The drying time varied between 2 and 16 h and was one of the adjustable parameters in this study.

In the second step, a PAAM gel slab was made between two glass slides, approximately 3.0–4.0 mm apart, with the NIPA network (~1.2 mm thick at its equilibrium swollen state) between them and in contact with one of the glass slides. The distance between the two glass slides was larger than was the thickness of the swollen NIPA network. The acrylamide gel "ingredient" that was allowed to diffuse into the NIPA network before polymerization was initiated to ensure better formation of the NIPA–PAAM interpenetrating networks. The diffusion time varied between 10 min and 24 h and was the second adjustable parameter. Then, the gelation was started by introducing an initiator (APS) into the PAAM pregel solution. The gelation occurred within about 15 min and was left overnight for completion.

The acrylamide gel consists of 700 m*M* acrylamide and 8.6 m*M* BIS. The end products are gel slabs 3.0–4.0 mm thick with a layered network structure: a PAAM network 1.8–2.8 mm thick and a 2.2-mm PAAM network interpenetrated by the NIPA network.

To expose the bigel interface, the samples were cut with different razor blades, steel wire 0.2 mm in diameter, and a sharp knife. After we checked that all three surface-preparation techniques gave similar results, we focused on using the steel wire to cut the specimen. The sample in the shape of a rectangular slab was placed in a glass vial filled with deionized and distilled water, the plane of the bigel's interface being orientated perpendicular to the vials' top and bottom surfaces. To prevent the bigels from floating in their aqueous environment and to keep them in a fixed position, the bigels were secured with Teflon hooks and spacers. To avoid water evaporation, the vial was sealed with a 100-$\mu$m-thick microscope slide. The gel was gently pressed against the slide, resulting in a plane surface, still leaving, however, a very thin water film between the gel and the coverglass. The vial was mounted onto

the $x$–$y$–$z$ positioning stage. The sample was advanced in both the $x$- and $y$-directions in steps of 2 $\mu$m, thereby mapping the concentration of the two polymers over an area of 100 by 100 $\mu$m. Scans measuring the extent of the interface were operated only in the $x$-direction in steps of 2 $\mu$m.

Raman spectra were obtained by illuminating the sample with an argon laser operating at the wavelength of 514 nm. The laser beam was focused by a 100× objective of a confocal microscope, Olympus BH2, 10 $\mu$m below the top surface of the gel. The spatial resolution in the lateral plane was about 1 $\mu$m and better than 4 $\mu$m along the optical axis. The light scattered from the gel tissue was collected by the same objective and the spectral analysis was done using an axial transmissive spectrograph (Kaiser Optical Systems, HoloSpec) equipped with a Princeton Instrument CCD camera. Raman spectra of the gels, in the frequency range between 300 and 2000 $cm^{-1}$, with a spectral resolution of 4.0 $cm^{-1}$, were obtained using a 2-s integration time. The spectra were analyzed using spectroscopic software, GRAM 32. The Raman scans were performed for several samples and they showed reproducible results. No attempt to obtain 3D maps was made.

## RESULTS AND DISCUSSION

A detailed analysis of the NIPA spectrum was given in our previous reports.[7,17] In these studies, we used the intensity of the 1455 $cm^{-1}$ band due to NIPA to monitor the density of this polymer near its interface with water. Please note that in refs. 7 and 17 we described the position of this band as 1445 $cm^{-1}$. By plotting the intensity of this peak, we obtained the contour map shown in Figure 1(a). It is seen that the boundary is not well defined and the polymer extends into the water to various depths. Although to the naked eye the surface looks smooth, Figure 1(a) clearly indicates that the surface is not homogeneous.

Experimental points obtained during linear scans [Fig. 1(a) is a contour map of a parallel set of such scan lines] were fitted to a Gaussian distribution function:

$$F(x) = c_1 + c_2\exp(-x^2/d^2), \quad (1)$$

where $x$ measures the linear displacement perpendicular to the interface and $d$, the penetration depth, is the fitting parameter. The penetration-depth parameter is a measure of the thickness of the interface at the location of the scan line. Equation (1) fitted the experimental data very well as shown in Figure 1(b). Because the interface is not uniform, different scans provided various $d$ values. At room temperature, the average water–NIPA interface thickness was found to be 37 ± 23 $\mu$m.

In this study, we focused on the 1455 $cm^{-1}$ peak due to both the NIPA and PAAM gels and the 1430 $cm^{-1}$ peak which is due to the $CH_2$ bending vibrations of the PAAM gels; compare Figure 2. These peaks were selected because they are well isolated from other bands and the background can be precisely determined. We assumed that the measured intensity is proportional to the concentration of the polymer within the focus of the laser. The doublet shown in Figure 2 has a complicated structure. Figure 2 shows the experimental contours and the components found by a fitting routine for two different locations near the interface. This procedure, however, is time-consuming and subject to subjective interpretation. Nevertheless, it was applied to a series of spectra and the intensity ratio of the NIPA and PAAM components allowed us to estimate the relative concentration of these components. A faster procedure, which proved to be equally accurate, is based on integrated intensities of the experimental maximums of the doublet:

$$I_{1455}/I_{1430} = (c_{\mathrm{NIPA}}I_{\mathrm{NIPA}} + c_{\mathrm{PAAM}}I_{\mathrm{PAAM}})/I_{\mathrm{PAAM}} = aI_{\mathrm{NIPA}}/I_{\mathrm{PAAM}} + b \quad (2)$$

where $a$ and $b$ are coefficients that depend on the polymer concentration and the magnitude of the transition dipole moment associated with the given vibration. Thus, a graph depicting the intensity ratio $I_{1455}/I_{1430}$ versus the position of the laser beam provides information on the distribution of the polymers within the system. An example of such a distribution is depicted in Figure 3. It is seen that the intensity ratio $I_{1455}/I_{1430}$ varies between 3 and 1. The minimum value of $b$ approximately equals 1 and corresponds to the relative intensity ratio of the two components of the PAAM doublet; compare Figure 2(b). The maximum value $b = 3$ was observed inside the NIPA substrate and was practically independent of the location. This value indicates that during the diffusion process the PAAM monomer solution could completely penetrate and fill out the pores and vacancies in the NIPA-gel sublayer. It is impor-

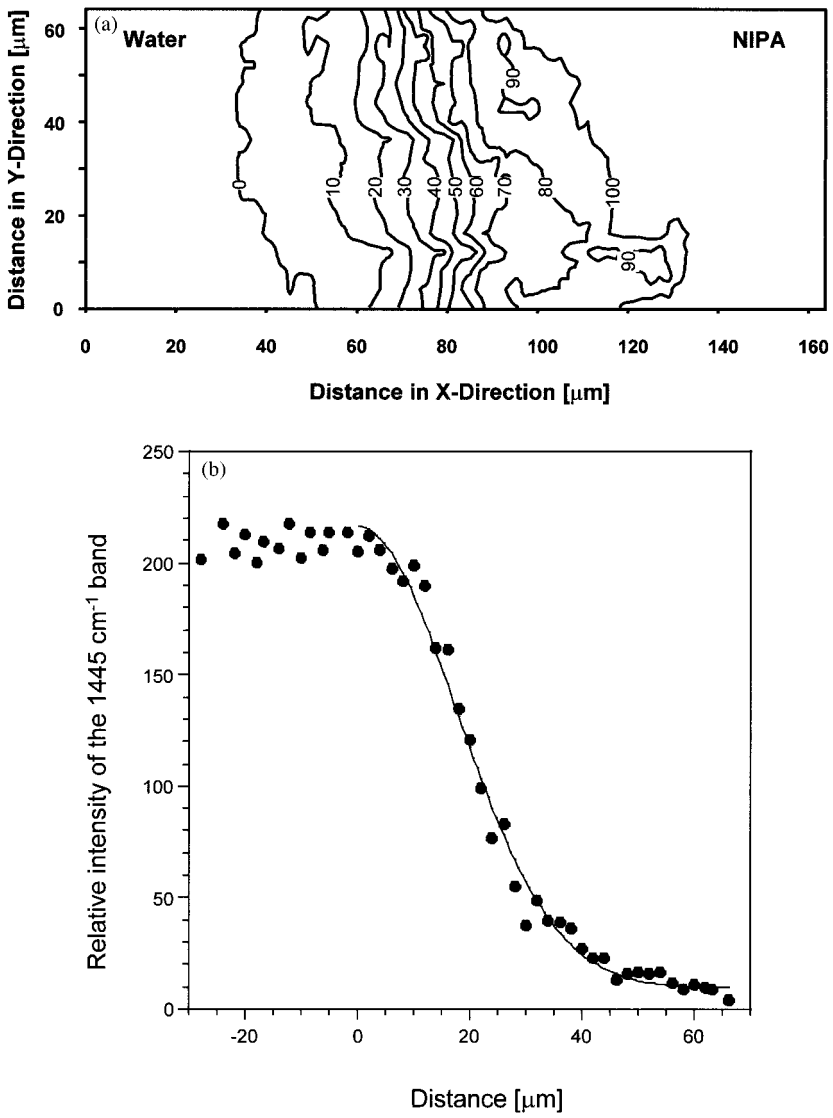


**Figure 1** (a) Contour map of Raman band intensity near 1455 $cm^{-1}$ of the NIPA polymer near the NIPA–water interface at 22°C. (b) Concentration of the NIPA polymer across the NIPA–water interface at 22°C. The solid line is a Gaussian function fitted to the experimental data. Penetration depth $d$ equals 34 microns.

tant to note that the maximum value $b = 3$ was observed for all bigels obtained according to the manufacturing protocols with more than 30 min of diffusion time.

This procedure of obtaining the concentration mapping was verified by using different pairs of Raman bands. Results were similar; however, we believe that analyzing the 1430–1455 $cm^{-1}$ doublet is more accurate, since these bands are in the region of a flat background. Other regions have slopping backgrounds and background corrections introduce significant error. It is important to note that both the fitting procedure and the integrated intensity ratio led to the same result.

One example of the intensity ratios, $I_{1455}/I_{1430}$, obtained along a linear scan, is shown in Figure 3. Those data were fitted to a Gaussian function, giving the penetration depth $d = 28$ microns. The average penetration depths, $d$, obtained for bigels fabricated under different synthesis conditions, are summarized in Table I. The estimated precision is about 20 %. By applying this procedure to larger scanning areas, we obtained contour plots for the interface between NIPA and PAAM, of which one is exhibited in Figure 4. The contour map for this interface is similar to that obtained for the pure NIPA–water interface [Fig. 1(a)]. For the bigels, the limits of the interface are not well

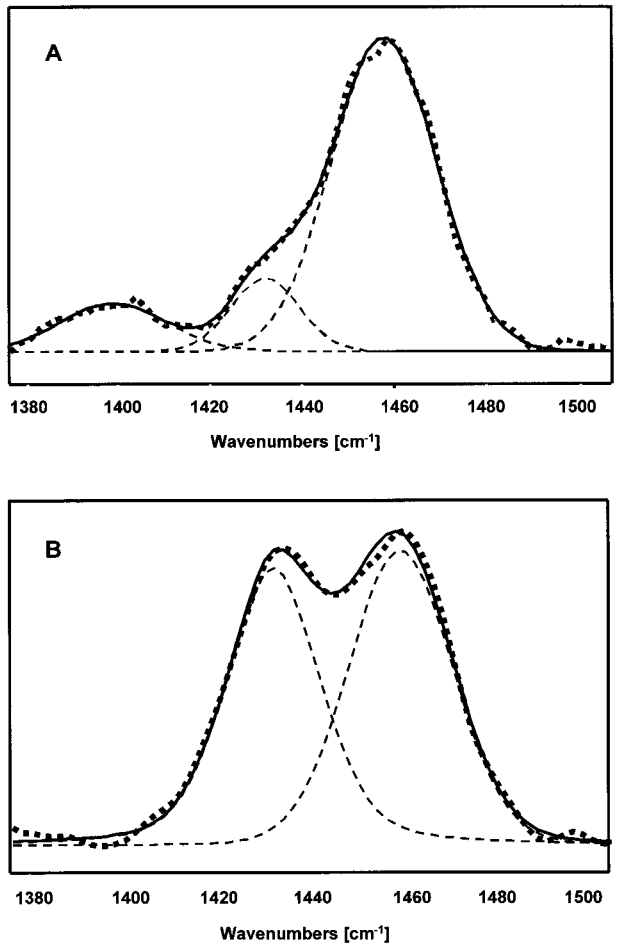


**Figure 2** Raman contours in the 1430- and 1455-$cm^{-11}$ frequency range for a bigel interface; (solid line) the fitted contour. Resolved components are shown as dashed lines. (A) Spectrum recorded at the "NIPA side" of the interface; (B) spectrum recorded at the "PAAM side" of the interface.

defined and the NIPA polymer extends into the PAAM gel to various depths, indicating that the interface is not homogeneous.

Two factors may determine the penetrating depth of the PAAM gel into the NIPA network: (1) evaporation of water from the NIPA network during the drying process which roughens the surface of the substrate, and (2) diffusion of PAAM into the NIPA gel. In one series of experiments, the diffusion time, in which the PAAM solution could penetrate the NIPA substrate, was allowed to vary, but all other parameters remained fixed; in particular, the drying time was set to 2 h. The effect of the diffusion time was examined by comparing the values of the penetration depth $d$ obtained for various diffusion times used in the

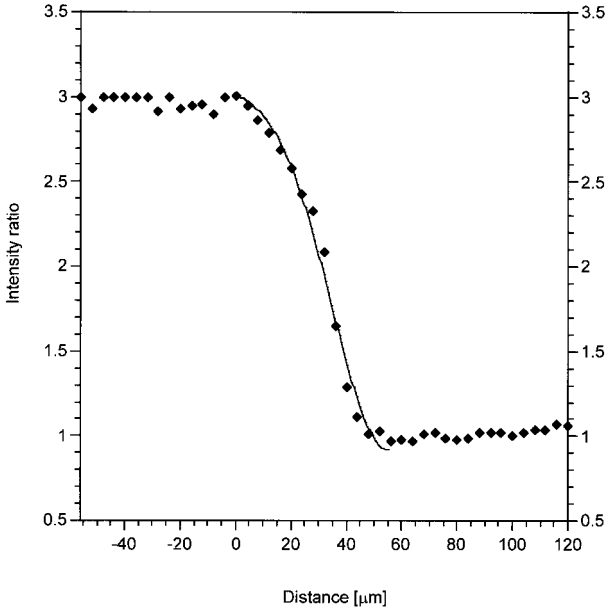


**Figure 3** Intensity ratio of the 1430 and 1455 $cm^{-11}$ bands across the interface. Diffusion time of the PAAM was 2 h; the substrate NIPA was dried for 3 h prior to diffusion. The solid line represents the best fit of eq. (1) to the experimental points. Penetration depth $d$ = 28 microns.

manufacturing protocol (see Table I). After an initial 30 min, no significant changes in the dimension of the interface were observed. Beyond

**Table I Average Thickness of the NIPA–PAAM Interface as a Function of the Preparation Method**

| NIPA Drying Time (Before the PAAM Diffusion) | PAAM Diffusion Time (h) | Transition Distance $D$ ($\mu$m) |
|---|---|---|
| 3 h | 1/6 | 16 |
| | 1/2 | 26 |
| | 2.0 | 27.5 |
| | 10.0 | 28.0 |
| | 24.0 | 26.5 |
| PAAM Diffusion Time | NIPA Drying Time (h) | Transition Distance $D$ ($\mu$m) |
| 2 h | 20 | 28 |
| | 3.0 | 27.5 |
| | 8.0 | 47.6 |
| | 16.0 | 156 |

The values of $D$ are averages of 7–10 linear scans.

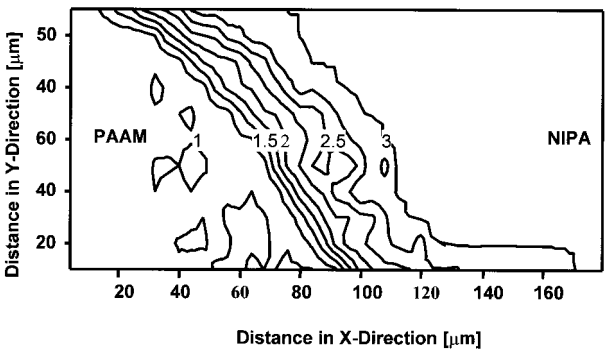


**Figure 4** Typical contour map of the Raman intensity ratio $I_{1455}/I_{1430}$ near the NIPA–PAAM interface at 22°C.

this time period, the average interface width for the bigel's transition zone did not exceed 27 $\mu$m.

While the width of the bigel transition zone seems to be independent of the diffusion time (as long as it is longer than 30 min), there is a strong correlation between the drying time of the NIPA ground layer of the bigel and the extension of the interface. When the drying times are short, the structure's NIPA surface does not change significantly and probably looks like the NIPA–water interface at room temperature. However, a longer drying of the NIPA gel results in an increased penetrating depth.

In the drying process, the NIPA sample is placed in a covered container with several holes so that water in the NIPA gel can slowly evaporate. The rate of evaporation depends on the temperature and the open area of the container. The higher the temperature, the greater the fraction of water molecules in the sample that have sufficient kinetic energy to break free from the surface of the gel and escape into the vapor. On the other hand, a larger opening results in faster evaporation and a rougher surface.

When the gel with the depleted surface layer was immersed into the PAAM pregel solution, the NIPA gel tends to swell by absorbing the PAAM solution. The time $\tau$ for the PAAM pregel solution to the NIPA gel involves deformation (swelling) of the NIPA network and, thus, is determined by a collective diffusing process.[18] $\tau$ can be generally described by a scaling relation:

$$\tau = a^2/D \tag{3}$$

where $a$ is the initial (shortest) linear size of the gel, and $D$, the effective collective diffusion coefficient. Considering the top layer as a large disk with depth $a$, $D$ is related to the diffusion constant ($D_0$) for a spherical gel and the elastic moduli (both the bulk modulus $K$ and the shear modulus $\mu$) and friction coefficient $f$ between water and the gel network:

$$D = \frac{1}{3} D_0 = \frac{K + \frac{4}{3}\mu}{3f} \tag{4}$$

Using $D_0 \approx 2.0 \times 10^{-7}$ cm$^2$/s (ref. 19) at room temperature, and assuming that $a \approx d = 28$ $\mu$m, we obtain $\tau \approx 2$ min. This estimation is good as long as the deformations are small. It is therefore not surprising that there is a large disagreement between the expected experimental value. For a thicker depletion layer, the scaling relation will no longer hold. Also, the bulk modulus and shear modulus will change for highly dehydrated gels. Generally, $K$ and $\mu$ become larger, resulting in a larger $D$. These effects may explain why the interface continues to grow until the diffusion times reaches 30 min. For a very long drying time of 16 h, extended pores were formed and the PAAM solution was absorbed quickly to fill the dehydrated surface layer.

## CONCLUSIONS

This study has shown that Raman microscopy is a powerful tool for the investigation of the polymer concentration distribution across the transition zone of an NIPA–PAAM bigel. Unlike many other imaging techniques, Raman spectroscopy allows chemical mapping not only from the sample's surface, thus providing data concerning the surface roughness, but also from within the bulk system, like the bigel's interface. The results proved the assumption that different drying and diffusion times have an impact on the topography of the interfacial region, where the two different gel slides are fitted together. It was believed that longer diffusion times result in more extended interfaces. We showed, however, that no further changes in the process of the PAAM pregel solution penetrating into the NIPA pore network are observed beyond 30 min of diffusion time. This result is of importance for a time-efficient synthesis process of the bigels.

The authors acknowledge the Donors of the Petroleum Research Fund, administered by the American Chemical Society, and the U.S. Army Research Office (Grant No. DAAH04-93-G-0215) for support of this research.

## REFERENCES

1. Hoffman, A. S. Macromol Symp 1996, 101, 443–454.
2. Radner, B. D.; Hoffman, A. S. In Biomaterials Science; Ratner, B. D.; Hoffman, A. S.; Schoen, F. J.; Lemons, J. E., Eds; Academic Press: San Diego, 1996; pp 21–35.
3. Peppas, N. A. Hydrogels in Medicine and Pharmacy; CRC: Boca Raton, FL, 1987.
4. Nagorski, H. In Superabsorbent Polymers: Science and Technology; Buchholz, F. L; Peppas, N. A., Eds.; ACS Symposium series 573; ACS: Washington, D.C., 1994; pp 99–111.
5. Park, T. G.; Hoffman, A. S. Biotechnol Prog 1994, 10, 32.
6. Appel, R.; Xu, W.; Zerda, T. W.; Hu, Z. Macromolecules 1998, 31, 5071.
7. Appel, R.; Zerda, T. W.; Wang, C. J.; Hu, Z. Polymer, in press
8. Hu, Z.; Zhang, X.; Li, Y. Science 1995, 269, 525.
9. Zhang, X.; Hu, Z.; Li, Y. J Chem Phys 1996, 105, 3794.
10. Li, Y.; Hu, Z.; Chen, Y. J Appl Polym Sci 1997, 63, 1173.
11. Shiga, T.; Hirose, Y.; Okada, A.; Kurauchi, T. J Appl Polym Sci 1992, 44, 249.
12. Zhang, X.; Li, Y.; Hu, Z.; Littler, C. L. J Chem Phys 1995, 102, 551.
13. Li, Y.; Tanaka, T. Annu Rev Mater Sci 1992, 22, 243.
14. Shibayama, M.; Tanaka, T. Adv Polym Sci 1993, 109, 1.
15. Schild, H. G. Prog Polym Sci 1992, 17, 163–249.
16. Hirotsu, S.; Hirokawa, Y.; Tanaka, T. J Chem Phys 1987, 87, 1392.
17. Bansil, R.; Gupta, M. J Ferroelect 1980, 30, 63.
18. Li, Y.; Tanaka, T. J Chem Phys 1990, 92, 1365–1371.
19. Sato Matsuo, E.; Tanaka, T. J Chem Phys 1988, 89, 1695–1703.